

Actuating a Simple 3D Passive Dynamic Walker

Russ Tedrake

Computer Science and
Artificial Intelligence Lab

Massachusetts Institute of Technology
Cambridge, MA 02139
Email: russt@ai.mit.edu

Teresa Weirui Zhang, Ming-fai Fong

Department of
Mechanical Engineering

Massachusetts Institute of Technology
Cambridge, MA 02139
Email: {resa, flamingo}@mit.edu

H. Sebastian Seung

Howard Hughes Medical Institute
Brain & Cognitive Sciences

Massachusetts Institute of Technology
Cambridge, MA 02139
Email: seung@mit.edu

Accepted to IEEE International Conference on Robotics and Automation, 2004. DRAFT: Please do not circulate.

Abstract— The passive dynamic walker described in this paper is a robot with a minimal number of degrees of freedom, but which is still capable of stable 3D dynamic walking. First, we present the reduced-order dynamic models that we used to tune the characteristics of the robot’s gait. Then we present an actuated version of the robot and some preliminary active control strategies. The control problem for the actuated version of the robot is interesting because although it is theoretically challenging (4 degrees of under-actuation), the mechanical design of the robot made it relatively easy to create controllers which allowed the robot to walk stably on flat terrain and even up a small slope.

I. INTRODUCTION

In the late 1980’s, Tad McGeer [1], [2] introduced a class of walking robots, known as *passive dynamic walkers*, which walk stably down a small decline without the use of any motors. The most impressive passive dynamic walker [3] has knees and arms, and walks with a surprisingly anthropomorphic gait. As a whole, these machines provide an elegant illustration of how proper machine design can generate stable and potentially very energy efficient walking. The ideas, however, are only now beginning to have an impact on the way in which fully actuated bipedal robots are designed and controlled (i.e., [4], [5]).

To bridge the gap between passive and active walkers, a number of researchers have considered the problem of adding a small number of actuators to an otherwise passive device [6], [7], [8]. There are two major advantages to this approach. First, actuating a few degrees of freedom on an otherwise passive walker is a possible way to capitalize on the energy efficiency of passive walking and the robustness of actively controlled systems. Second, by allowing the dynamics of the system to solve a large portion of the control problem, it may be possible to simplify the control problem that needs to be solved by the actuators.

The goal of this paper is to describe the mechanical design of our simple 3D passive dynamic walker, and the design of some preliminary active control strategies that have been applied to a partially-actuated version of that robot. These relatively simple controllers allow the robot to walk on flat terrain, and even up a small slope.

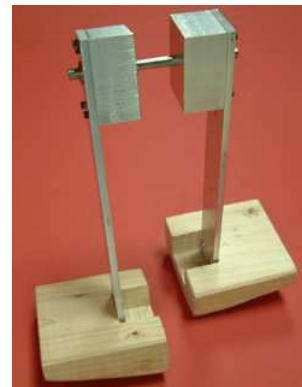


Fig. 1. The Passive Walker

II. PASSIVE DYNAMIC WALKER

The passive dynamic walker shown in Figure 1 represents the simplest machine that we could build which captures the essence of stable dynamic walking in three dimensions. It has only a single passive pin joint at the hip. When placed at the top of a small ramp and given a small push sideways, the walker will rock onto a single stance leg, allowing the opposite leg to leave the ground and swing forward down the ramp. Upon landing, the robot rocks onto the opposite foot, and the cycle continues. A number of videos have been included in the proceedings.

The energetics of this passive walker are common to all passive walkers: the energy lost due to inelastic collisions when the swing leg returns to the ground are balanced by the gradual conversion of potential energy into kinetic energy as the walker moves down the slope. The particular challenge for this walker was the design of the large curved feet. Using only reduced planar models of the dynamics, we were able to design feet which tuned the step frequency of the robot sufficiently well to produce an elegant and robust gait.

A. Frontal Plane Model

To model the dynamics in the frontal plane, we assume that the robot is always in contact with the ground at exactly one point and that the foot rolls without slipping. The equations of motion, in terms of body angle θ , for this planar model are

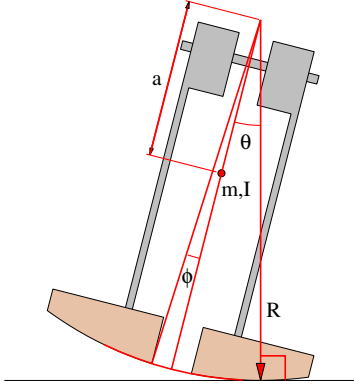


Fig. 2. Frontal Plane Model

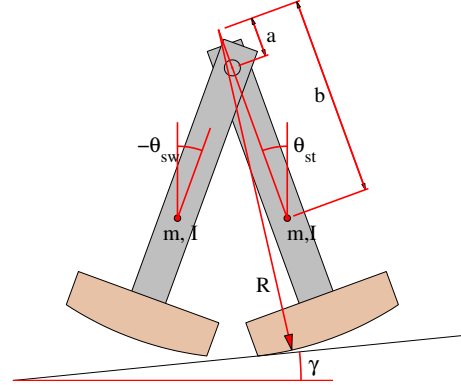


Fig. 3. Sagittal Plane Model

given in three parts using the form

$$H(\theta)\ddot{\theta} + C(\theta, \dot{\theta})\dot{\theta} + G(\theta) = 0.$$

When $|\theta| > \phi$, the ground contact point is in the curved portion one of the feet (the boundary condition on the outside of the foot is not modeled), and the dynamics are:

$$\begin{aligned} H(\theta) &= I + ma^2 + mR^2 - 2mRa \cos \theta, \\ C(\theta, \dot{\theta}) &= mRa\dot{\theta} \sin \theta, \\ G(\theta) &= mga \sin \theta. \end{aligned}$$

When $|\theta| \leq \phi$, the ground contact is along the inside edge of the foot. In this case, the dynamics are:

$$\begin{aligned} H(\theta) &= I + ma^2 + mR^2 - 2maR(\cos \theta \cos \alpha + \sin \theta \sin \alpha), \\ C(\theta, \dot{\theta}) &= 0, \\ G(\theta) &= mg(a \sin \theta - R \sin \alpha). \end{aligned}$$

where $\alpha = \theta - \phi$ if $\theta > 0$, otherwise $\alpha = \theta + \phi$.

Finally, the collision of the swing leg with the ground is modeled as an inelastic (angular momentum conserving) impulse,

$$\dot{\theta}^+ = \dot{\theta}^- \cos \left[2 \tan^{-1} \left(\frac{R \sin \phi}{R \cos \phi - a} \right) \right],$$

which occurs when $\theta = 0$.

The actuated version of the robot, presented in section III, carries its mass very differently than the purely passive version of the robot, due to the added mass motors and sensors. By simulating this model, we were able to find very different radii for the feet in the frontal plane that allowed the different versions of the robot to both oscillate back and forth at the desired frequency of approximately 1.4Hz.

B. Sagittal Plane Model

In the sagittal plane, the dynamics are a slightly modified version of the well-studied compass gait [9]. The parameters of this model can be found in Figure 3, and the dynamics are given by:

$$\mathbf{H}(\mathbf{q})\ddot{\mathbf{q}} + \mathbf{C}(\mathbf{q}, \dot{\mathbf{q}})\dot{\mathbf{q}} + \mathbf{G}(\mathbf{q}) = \mathbf{0},$$

where $\mathbf{q} = [\theta_{st}, \theta_{sw}]^T$, and:

$$\begin{aligned} H_{11} &= I + m(b \cos \theta_{st} - R \cos \gamma)^2 + m(b \sin \theta_{st} - R \sin \gamma)^2 \\ &\quad + m(a \cos \theta_{st} - R \cos \gamma)^2 + m(a \sin \theta_{st} - R \sin \gamma)^2, \\ H_{12} = H_{21} &= m(a \cos \theta_{st} - R \cos \gamma)((b - a) \cos \theta_{sw}) \\ &\quad + m(a \sin \theta_{st} - R \sin \gamma)((b - a) \sin \theta_{sw}), \\ H_{22} &= I + m((b - a) \sin \theta_{sw})^2, \\ C_{11} &= mR(b + a)\dot{\theta}_{st}(\sin \theta_{st} \cos \gamma - \cos \theta_{st} \sin \gamma) \\ &\quad + \frac{1}{2}ma(b - a)\dot{\theta}_{sw}(\sin \theta_{st} \cos \theta_{sw} - \cos \theta_{st} \sin \theta_{sw}), \\ C_{12} &= m(b - a)\dot{\theta}_{sw} \cos \theta_{sw} \left(\frac{a}{2} \sin \theta_{st} - R \sin \gamma \right) \\ &\quad - m(b - a)\dot{\theta}_{sw} \sin \theta_{sw} \left(\frac{a}{2} \cos \theta_{st} - R \cos \gamma \right) \\ &\quad - \frac{1}{2}ma(b - a)\dot{\theta}_{st}(\sin \theta_{st} \cos \theta_{sw} - \cos \theta_{st} \sin \theta_{sw}), \\ C_{21} &= ma(b - a)\dot{\theta}_{st}(\sin \theta_{st} \cos \theta_{sw} - \cos \theta_{st} \sin \theta_{sw}) \\ &\quad - \frac{1}{2}m(b - a)\dot{\theta}_{sw} \cos \theta_{sw} (a \sin \theta_{st} - R \sin \gamma) \\ &\quad + \frac{1}{2}m(b - a)\dot{\theta}_{sw} \sin \theta_{sw} (a \cos \theta_{st} - R \cos \gamma) \\ C_{22} &= \frac{1}{2}m(b - a)\dot{\theta}_{st} \cos \theta_{sw} (a \sin \theta_{st} - R \cos \gamma) \\ &\quad - \frac{1}{2}m(b - a)\dot{\theta}_{st} \sin \theta_{sw} (a \cos \theta_{st} - R \cos \gamma) \\ &\quad + m(b - a)^2 \dot{\theta}_{sw} \sin \theta_{sw} \cos \theta_{sw} \\ G_1 &= mg(a + b) \sin \theta_{st} - 2mgR \sin \gamma, \\ G_2 &= mg(b - a) \sin \theta_{sw}. \end{aligned}$$

The abbreviation *st* stands for the stance leg, and *sw* for the swing leg.

The primary determinant of step length and forward velocity is the slope of the ground, γ . Our robot walks on a small treadmill with an actuated incline. The curvature of the feet in the sagittal plane should be set so that the pendular period of the system approximately matches the step frequency from the frontal model.

C. Experiments

Using a 1.4Hz step frequency as a target, the planar models can be used to find values for the radius of curvature of the feet in the frontal (R_f) and sagittal (R_s) planes. We constructed experimental feet using a CNC milling machine to cut out the surface given by:

$$z = \sqrt{R_f^2 - x^2} - R_f + \sqrt{R_s^2 - y^2} - R_s.$$

Using these feet, this simple passive structure produces *stable* periodic trajectories when the robot is placed on a small decline. Figure 4 plots some sample trajectories of model walking down a slope of 0.035 radians which demonstrate this stability. θ_{roll} is the roll angle of the body of the robot, in radians, which was simply called θ in the frontal plane model.

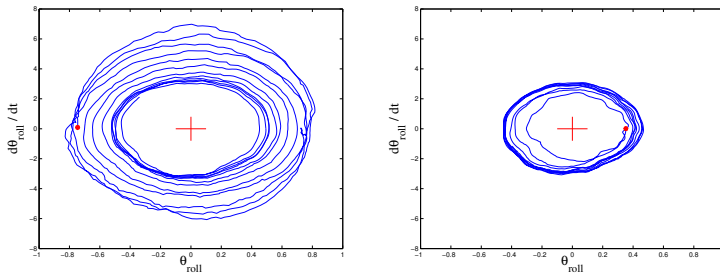


Fig. 4. Experimental Limit Cycles. The limit cycles are plotted in phase space, with cross hairs at the origin and a dot at the initial conditions of the robot. The first plot shows the recovery from large initial conditions, and the second shows recovery from small initial conditions.

There are a number of aspects of the walking that are not captured by the planar models. The frontal and sagittal plane dynamics are actually coupled; converted potential energy from the sagittal plane is used to stabilize the oscillations in the frontal plane, as Figure 4 illustrates. Also, the swing leg creates an uncompensated moment about the z -axis, which occasionally causes the robot to twist and change direction, making it walk across the ramp instead of down it. This yaw moment can potentially be compensated for by adding arms to the robot [3]. Finally, the robot is attached to the computer and power supply via a tether. Because the robot is so light, the tether can actually have a significant impact on the dynamics, acting almost as a leash on the robot.

D. Stability

Traditionally, the local stability of the passive walkers is quantified by examining the eigenvalues of the linearized step-to-step return map [1], taken around a point in the period either immediately preceding or immediately following the collision. The sensors on our robot do a poor job of sensing the impact, but we have evaluated the return map through the hyperplane when $\theta_{roll} = 0$. This is the point in the cycle when the robot passes through the vertical position in the frontal plane, which is the expected point of impact. By evaluating the return map over a small number of recorded trials when the robot walked

straight down the ramp, the largest eigenvalue, $\max|\lambda|$, was found to be approximately 0.8.

In practice, the robot is quite stable to large perturbations in the frontal plane when they add energy into the system. Very large perturbations cause the robot to tip over sideways. The robot has a stable fixed point at $\theta_{roll} = \dot{\theta}_{roll} = 0$, so large perturbations which remove energy from the system often cause the robot to come to a standstill. Large perturbations in the sagittal plane often caused the robot to fall over forward or backward. Walking trials were nearly always started with the legs at the same absolute angle. It was not necessary to give the robot any initial forward velocity.

III. TODDLER - THE ACTUATED VERSION

In order for the robot to walk on the flat, it must actively restore the energy lost during impact. One candidate active control strategy would be to apply torques at the existing hip joint, but it may be difficult to actuate the hip without disrupting the basic passive gait. On the robot shown in Figure 7, the hip joint is passive, but we have added two active joints (pitch and roll) at each ankle. We call this robot “Toddler” for two reasons. First, the word toddler is normally used to describe a child during the time that they are learning to walk, and this robot was primarily designed to investigate learning algorithms for dynamic walking. The name is also appropriate because the robot literally toddles back and forth when it walks.

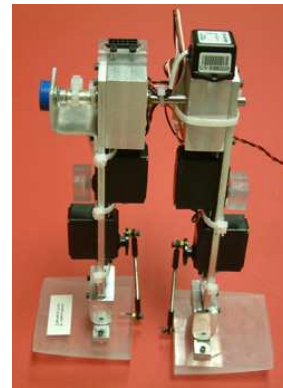


Fig. 5. The Toddler Robot

Toddler’s four active degrees of freedom are actuated by servo motors through mechanical linkages. They are configured so that when the motors are commanded to hold their zero position, the robot simulates the passive walker. The robot is also equipped with a two axis (pitch and roll) gyroscopic tilt sensor and a potentiometer at the hip to measure the relative hip angle. The control algorithms are run on an embedded PC/104 stack with a 700 MHz processor.

By assuming that the robot is always in contact with the ground, we can describe the generalized state of this robot with eight variables - body yaw, pitch, and roll, the relative hip angle, and pitch and roll for the two ankles - plus their derivatives. Because the robot only has four actuators, is

clearly an under-actuated system. The challenge is to produce a control strategy for the ankle actuators which (directly or indirectly) controls all eight degrees of freedom.

IV. STABILIZING FRONTAL PLANE OSCILLATION

The planar model was a simplification of the dynamics when the robot was on a ramp, but it is a reasonable representation of the robot's dynamics when it is placed on a flat surface. The frontal plane model for the actuated version can be written as:

$$\mathbf{H}(\mathbf{q})\ddot{\mathbf{q}} + \mathbf{C}(\mathbf{q}, \dot{\mathbf{q}})\dot{\mathbf{q}} + \mathbf{G}(\mathbf{q}) = \mathbf{u},$$

where $\mathbf{q} = [\theta, \theta_{la}, \theta_{ra}]^T$ and $\mathbf{u} = [0, u_{la}, u_{ra}]^T$. The abbreviations *la* and *ra* are short for left and right ankle, respectively. The impact model can be written as

$$\dot{\mathbf{q}}^+ = \mathbf{\Omega}(\mathbf{q})\dot{\mathbf{q}}^-.$$

At each collision with the ground, the kinetic energy of the system, T , changes by:

$$\Delta T = \frac{1}{2}\dot{\mathbf{q}}^T [\mathbf{\Omega}(\mathbf{q})^T \mathbf{H}(\mathbf{q}) \mathbf{\Omega}(\mathbf{q}) - \mathbf{H}(\mathbf{q})] \dot{\mathbf{q}}.$$

In order to stabilize the oscillations in the frontal plane, the control torques, \mathbf{u} , must restore the energy lost from these collisions. In the following sections, we will discuss two simple actuation strategies that have already been applied successfully to the robot.

A. Feed Forward Ankle Trajectories

The ankle servos are PD controllers which follow a reference trajectory. The first actuation strategy that we experimented involved playing out a feed forward trajectory which applied a periodic drive to the robot's ankles:

$$\begin{aligned} \theta_{ra}^d &= \alpha \sin(2\pi\omega t) \\ \theta_{la}^d &= -\theta_{ra}^d \end{aligned}$$

Whether or not the robot's dynamics could entrain to the dynamics of the controller depended on the relationship between the controller's frequency, ω , and the passive step frequency of the robot. Surprisingly, the best entrainment occurred when the controller was a little slower than the passive step frequency. The entrained robot took such large, slow steps that one believes that the robot will eventually be able to navigate rough or intermittent terrain. We believe that the success of this simple controller can be attributed to the mechanical design of the robot.

Local stability analysis of the limit cycles generated by the feed forward controller suggests that they are slightly more stable than the purely passive limit cycles, $\max |\lambda| \approx 0.72$. Even this number may be artificially high, because the trajectories appear to mostly converge within 2 cycles, but there is a lot of noise around the converged trajectories. Practically, this controller is not very stable because any sizable disturbance will knock it off the cycle.

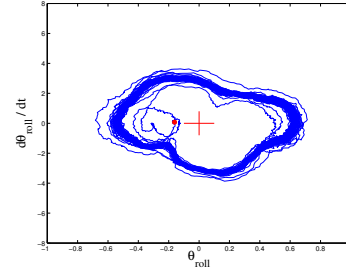


Fig. 6. Example Feed forward Limit Cycle

B. Feedback Ankle Trajectories

A more direct approach to stabilizing the roll oscillations is to build a controller which, on every cycle, injects the same amount of energy back into the system that was lost during that cycle. Unfortunately, due to the limitations of the sensor hardware on the robot, it is difficult to measure exactly the amount of energy lost at the time of each collision. The actuators of the robot are driven through a PD position control board, so it is also difficult to inject a very specific amount of energy into the system.

Instead of modeling the energy from the sensors and generating a corresponding torque at the ankle, we have implemented a feedback control strategy inspired by Marc Raibert's height controller [10] for hopping robots. The idea is to inject an approximately constant amount of energy into the system during every cycle. The system will settle into a stable oscillation with an amplitude that is monotonically related to the energy injected. The amplitude can then be tuned experimentally by changing the amount of energy injected into the system. An analysis of this idea can be found in [11].

The heuristic for injecting a roughly constant amount of energy on each cycle is as follows. As the robot rotates from an upright position onto one foot, it will cross a threshold position at which the stance ankle is servo-ed by a small fixed amount, causing the robot to accelerate further in the direction that it was moving. As the robot is moving back toward the upright position and it crosses that threshold again, the ankle is servo-ed back to the original, zero position, which further accelerates the robot toward the upright position. It is important that both ankles be at the zero position at $\theta_{roll} = 0$ in order to minimize the energy lost by the collision with the ground.

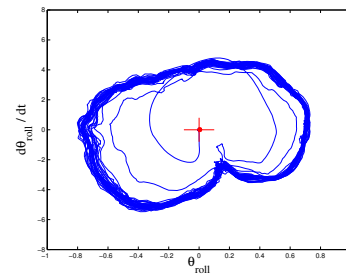


Fig. 7. Example Feedback Limit Cycle

The local stability analysis of this controller, $\max |\lambda| \approx$

0.68, reveals that this controller converges faster than the open-loop controller and faster than the purely passive trajectory. Practically, this controller is very stable. It is able to recover from very large disturbances, and from very small initial conditions.

V. VELOCITY CONTROL

The robot walks in place when the center of mass of the entire robot is directly above the point of contact between the foot and the ground. When the center of mass is out in front of the ground contact point, the robot will lean forward. As soon as one leg leaves the ground, the passive joint at the hip allows it to swing forward, and the robot begins walking. This happens naturally when the robot is on an incline. The farther the center of mass is from the ground contact point, the faster the robot will move in that direction. On Toddler, the operator specifies the desired forward speed by joystick, and the corresponding placement of the center of mass is controlled by actuating the ankle pitch actuators. The heuristic makes it easy for Toddler to walk on flat terrain, and even up small inclines.

The direction of the robot can also be controlled, to a limited degree, by differentially actuating the right and left ankles (either pitch or roll). Currently, the yawing of the robot due to momentum of the swing leg and slipping on the stance leg limit the controllability of the robot's heading. Future versions of the robot will have arms to compensate for this yaw, and should be able to turn more accurately.

VI. CONCLUSIONS AND FUTURE WORK

The passive dynamic walker presented in this paper has only a few degrees of freedom, but it is capable of stable 3D dynamic walking. The dynamics are simple enough that they can be fully modeled and understood. We have presented the preliminary modeling work, which considered the frontal and sagittal planes individually, and are currently studying the three dimensional dynamics to better understand the coupling terms.

The control problem for the Toddler robot is interesting because although it is theoretically challenging (4 degrees of under-actuation), the mechanical design of the robot made it relatively easy to create controllers which allowed the robot to walk stably on flat terrain and even up a small slope. This feature of the robot makes it an excellent platform for studying machine learning control strategies, which is the true focus of our project. In the future, we would also like to implement more elegant model-based, under-actuated control strategies that might allow for improved active control of step length and stride frequency, and possibly allow the robot to walk over rough or intermittent terrain.

ACKNOWLEDGMENTS

This work was supported by the David and Lucille Packard Foundation (contract 99-1471), the National Science Foundation (grant CCR-0122419), Howard Hughes Medical Institute, and the MIT Undergraduate Research Opportunities Program.

REFERENCES

- [1] T. McGeer, "Passive dynamic walking," *International Journal of Robotics Research*, vol. 9, no. 2, pp. 62–82, April 1990. [Online]. Available: Mcgeer90.pdf
- [2] T. McGeer, "Passive walking with knees." IEEE Conference on Robotics and Automation, 1990, pp. 1640 – 1645. [Online]. Available: Mcgeer90a.pdf
- [3] S. H. Collins, M. Wisse, and A. Ruina, "A three-dimensional passive-dynamic walking robot with two legs and knees," *International Journal of Robotics Research*, vol. 20, no. 7, pp. 607–615, July 2001. [Online]. Available: Collins01.pdf
- [4] J. Pratt, "Exploiting inherent robustness and natural dynamics in the control of bipedal walking robots," Ph.D. dissertation, 2000. [Online]. Available: Pratt00.pdf
- [5] M. W. Spong and G. Bhatia, "Further results on control of the compass gait biped." International Conference on Intelligent Robots and Systems, 2003, pp. 1933–1938. [Online]. Available: Spong03.pdf
- [6] J. Camp, "Powered "passive" dynamic walking," Master's thesis, 1997. [Online]. Available: Camp97.pdf
- [7] R. Q. van der Linde, "Active leg compliance for passive walking." IEEE International Conference on Robotics and Automation (ICRA), 1998, pp. 2339–2345. [Online]. Available: VanDerLinde98.pdf
- [8] A. D. Kuo, "Energetics of actively powered locomotion using the simplest walking model," *Journal of Biomechanical Engineering*, vol. 124, pp. 113–120, 2002. [Online]. Available: Kuo02.pdf
- [9] A. Goswami, B. Espiau, and A. Keramane, "Limit cycles and their stability in a passive bipedal gait." IEEE Conference on Robotics and Automation, 1996, pp. 246 – 251. [Online]. Available: Goswami96.pdf
- [10] M. H. Raibert, *Legged Robots That Balance*. The MIT Press, 1986.
- [11] M. Buehler and D. E. Koditschek, "Analysis of a simplified hopping robot." IEEE Conference on Robotics and Automation, 1988, pp. 817–819. [Online]. Available: Buehler88.pdf